Fundamental assessment of oscillatory performance of grid-forming integrated systems

Sander Skogen
Intelligent Electrical Power Grids
Delft University of Technology
Delft, The Netherlands
Sanderskoge@gmail.com

Jose Rueda Torres
Intelligent Electrical Power Grids
Delft University of Technology
Delft, The Netherlands
j.ruedatorres@tudelft.nl

Peter Palensky
Intelligent Electrical Power Grids
Delft University of Technology
Delft, Netherlands
P.Palensky@tudelft.nl

***Abstract*—Electrical power systems are witnessing a paradigm shift from traditional synchronous generators towards an increased integration of power electronic interfaced (PEI) generation. As the global community leans towards renewables, ensuring grid stability during this transformation becomes paramount. This paper presents a fundamental study of oscillatory stability dynamics for three emerging grid-forming converter controller topologies: Virtual Synchronous Machine (VSM), droop control, and the Synchroverter, in comparison to conventional synchronous generation. Utilizing the two area 4 generator (2A4G) system for analysis, the research underscores the significance of converter integration, proximity-based enhancements in damping capabilities, and the delicate equilibrium in parameter tuning for optimal stability. The results pave the way for informed decision-making in grid development and renewable energy comprehension, highlighting the potential of grid-forming converter controllers in steering a sustainable energy future.**

***Index Terms*—Grid-Forming Converters, Oscillatory Stability, DigSilent PowerFactory, VSM, Droop, Synchroverter.**

I. Introduction

ELECTRICAL power systems are undergoing a transformative shift from the dominance of traditional synchronous generators to a paradigm characterized by a prolific integration of renewable energy sources governed by power electronic components [1]. Synchronous generators have historically supplied inherent benefits to the grid, such as inertia, synchronization, and damping torques, which facilitate system stability amidst dynamic perturbations [2]. However, power electronic interfaced (PEI) generation disrupts the direct grid linkage, thereby eliminating the innate stability attributes pivotal for dynamic system stability [3].

The International Renewable Energy Agency (IRENA) indicates that for the European Union (EU) to achieve its climate benchmarks, the renewable energy contribution to power generation should span 55 % by 2030 and surge to 86 % by 2050 [4]. Although PEI generation will not entirely encapsulate this transition, the escalating adoption of solar PV and wind energy amplifies its significance, especially with nations such as Denmark periodically achieving a complete reliance on PEI generation [5]. As such, the meticulous analysis of power electronic control becomes indispensable to ensure the harmonious merging of escalating renewable penetration with regard to power system stability.

Subsequent to the PEI generation influx, there has been an innovative surge in converter controllers, namely grid-forming controllers. Distinct from the conventional grid-following, which remains contingent upon a proximate grid, grid-forming controllers exhibit the versatility to operate autonomously or in tandem with a grid, expanding their control horizons [6]. While they offer a plethora of advantages, including black-start capabilities, resilience during weak-grid connections, and an array of ancillary services, they also grapple with challenges such as elevated costs, lagged power responses, and certain regulatory predicaments [7], [8]. While much of the prior research has explored these controller topologies, the primary focus has been on tuning the individual controllers. This paper, in contrast, offers a comparative analysis grounded in both analytical and time domain simulations [9]–[12].

Recognizing their pivotal role in increasing renewable penetration, this paper embarks on a comprehensive evaluation of three quintessential grid-forming converter controller topologies: the Virtual Synchronous Machine (VSM), droop control, and the synchroverter. These will be compared to traditional synchronous generation, analyzing the impact of the growing amount and location of this generation on system stability, both small-signal and transient, and offering potential measures to improve these. The system used in the analysis is the two area 4 generator (2A4G) system given in Fig. 1, highlighting the voltage levels, converter placement and generator type.

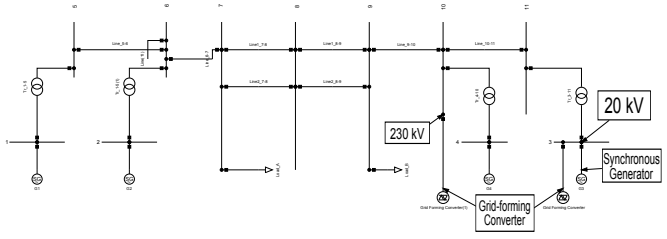

Fig. 1. System schematic in Powerfactory

Conclusively, this paper aims to highlight the inherent challenges associated with PEI generation, particularly concerning small-signal and transient stability. It aspires to provide pragmatic solutions to these challenges, strengthening the global strides towards a comprehensively renewable future. The work is done through modeling and simulations in DigSilent PowerFactory.

II. Modelling

This section explains the modeling of the three designated controllers.

A. Virtual Synchronous Machine

Virtual Synchronous Machines (VSM) aim to offer virtual inertia to the power grid, capturing the advantages of conventional inertia derived from traditional generation sources. This is accomplished by integrating short-term energy storage with a power inverter and a robust control system [13]. The essence of VSM is to emulate the inertia observed in traditional power generation, bridging the evolving grid to the extensively researched power system. In large generators, inertia functions as a reservoir of conserved energy, facilitating synchronism amongst generators. This inherent property of large machines ensures system stability before their control mechanisms introduce intended dynamic alterations [14]. Various VSM models have been proposed, each presenting distinct characteristics and modeling facets [13].

Fig. 2 present the control system of the VSM. The red highlight signifies the VSM control emulating the synchronous generator and its inertia. This emulation incorporates a revised swing equation, the inputs of which are derived from conventional synchronous generator formulas.

In terms of the swing equation:

$$\frac{2H}{\omega_0}\frac{d\omega}{dt} = P_m - P_e \tag{1}$$

It describes the interrelationship between power and the machine's acceleration, where $\frac{2H}{\omega_0}$ is the inertia constant. A perturbation in either mechanical or electrical power incites acceleration. The rate of this change hinges on the machine's cumulative inertia constant.

Within the VSM framework, the swing equation is altered to:

$$T_a s\omega = (P_{\text{ref}} - P) - D_p(\omega - \omega_{\text{ref}}) \tag{2}$$

Here, T_a stands for the acceleration time constant and D_p represents a damping coefficient. In essence, the operations of the controller predominantly rely on these two parameters.

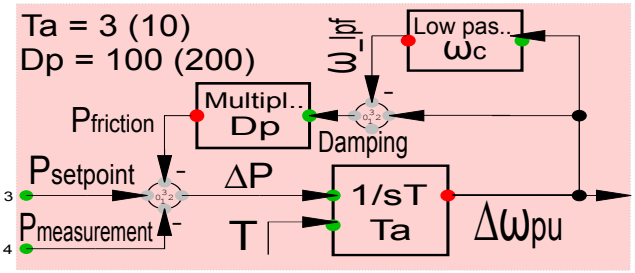

Fig. 2. VSM control block with given control parameters

B. Syncroverter Control

The syncroverter, similar to the VSM, derives its principles from the synchronous machine equations and the swing equation. One of the distinctions lies in the syncroverter's emphasis on torque over power, as utilized in VSM. Traditional synchronous generators that deploy a drooping frequency to regulate power output find a parallel in syncroverter control mechanisms. Specifically, it integrates both a frequency control loop centered around the converter's power and a voltage control loop focused on the reactive power.

In this context, the frequency control loop is highlighted in red and the voltage control loop in blue. Deriving from Equation 3, the frequency loop's governing equation is showcased in Fig. 4. Here, torque reference is determined by dividing power by the mechanical speed:

$$D_p = -\frac{\Delta T}{\Delta \theta} \tag{3}$$

$$T_a s\omega = (T_{\text{ref}} - T) - D_p(\omega - \omega_{\text{ref}}) \tag{4}$$

The voltage control loop employs the relationship detailed in Equation 5. This translates to the equation presented in the control system as Equation 6. The parameter D_q signifies the reactive power droop coefficient, with ΔQ and ΔV representing the variations in reactive power and voltage, respectively:

$$D_q = -\frac{\Delta Q}{\Delta v} \tag{5}$$

$$K_q = D_q(v_{ref} - v) + (Q_{ref} - Q) \tag{6}$$

Consequently, the pivotal parameters defining syncroverter control encompass the acceleration time constant T_a, the damping coefficient D_p, the voltage control gain K_q, and the reactive power droop coefficient D_q.

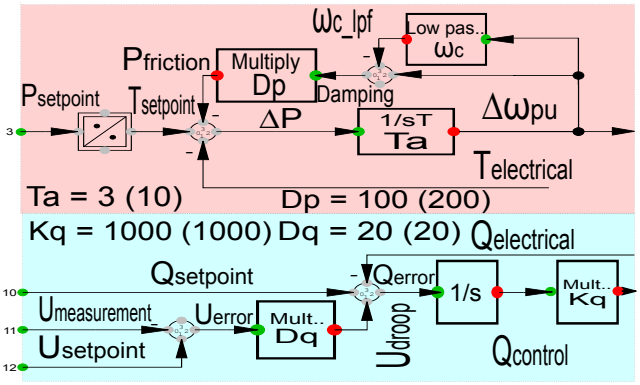

Fig. 3. Syncroverter control block with given control parameters

C. Droop Control Mechanism

The droop control approach employs a frequency-droop controller, initially conceptualized for the autonomous functioning of isolated microgrid systems [15]. Such a design ensures the controller operates without the need for communication, drawing parallels to traditional droop control methods found in synchronous generators. However, it does exhibit a slower transient response and suboptimal transient active power distribution [15]. Fig. 4 illustrates the control system, with power-frequency control highlighted in red and the reactive power-voltage control accentuated in blue.

In the power-frequency control framework, the governing equation is:

$$\Delta\omega = m_p \Delta P \tag{7}$$

Which translates into the control system as:

$$\omega_{gen} = \omega_{ref} - m_p(P_{out} - P_{in}) \tag{8}$$

Conversely, for the reactive power-voltage control:

$$\Delta v = m_q \Delta Q \tag{9}$$

Translating to:

$$V = V_{ref} - m_q(Q_{out} - Q_{in}) \tag{10}$$

In essence, the power-frequency control mechanism asserts that a frequency alteration directly correlates with a power change. Simultaneously, the reactive power-voltage control implies that voltage fluctuations directly correspond with alterations in reactive power.

Key control variables encompass m_p (active power droop coefficient) and m_q (reactive power droop coefficient).

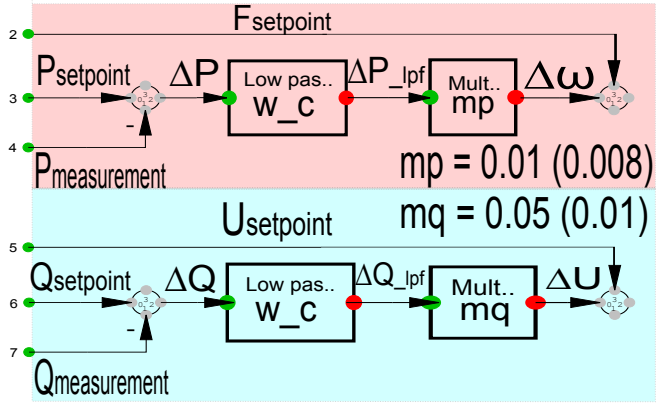

Fig. 4. Droop control block with given control parameters

III. Methodology

To analyze the different oscillatory performances of the system, different simulations were done. A scenario representing a 20 % load increment at Load A—symbolizing the demand in one of the dual sectors within the 2A4G framework—served as the perturbation for analysis. The foundational simulation parameters were adopted from the models in [15], as shown within the respective control block schematics.

The investigation comprised four distinct simulations. The initial simulation focused on the role of inertia in system stability. This phase entailed three separate simulations, each varying the inertia constants for generator G3 across three different magnitudes. Adopting a baseline of 900 MVA, the simulations explored an elevated scenario at 1200 MVA and a reduced scenario at 720 MVA, employing PowerFactory's integrated conversion metrics to utilize inertia constants of 45047.4 kgm^2, 60063.2 kgm^2, and 37539.5 kgm^2 for the trio of cases, respectively.

Subsequently, generator G3's output was moderated to 80 % of both active and reactive power, with the shortfall of 20 % being offset by the grid-forming converters. In this scenario, generator G3's inertia was set at 720 MVA.

The analysis then transitioned to evaluating the grid-forming converters' impact, simulating their operation independently at two pivotal junctures—initially at bus 3, followed by bus 10.

A sensitivity analysis was then done, utilizing the controller parameters as detailed in section II. This segment of the research offered a comparative exploration of how variances in these parameters influence system stability. Adjustments to the parameters were calibrated based on the specifications highlighted within the control block parentheses, situating the grid converters at bus 3 for this process.

To analyze the oscillatory behavior, eigenvalues and frequency oscillation plots generated through PowerFactory were instrumental. The eigenvalue analysis pinpointed the three most critical modes alongside frequency oscillations, implementing a nuanced understanding of system stability throughout the investigation.

A schematic representation of the research methodology is provided in Fig.5, offering a streamlined visual summary of the investigative process.

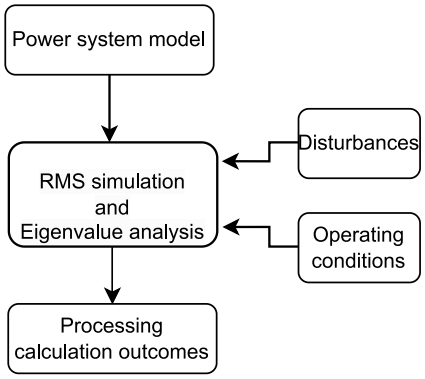

Fig. 5. Methodology flowchart

IV. Results

A. Inertia effects on Stability

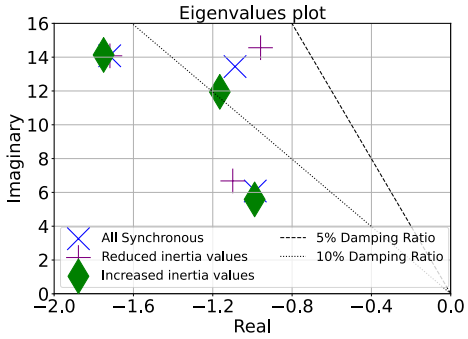

Fig. 6. Eigenvalues plot representing increased and reduced level of inertia during pertubation

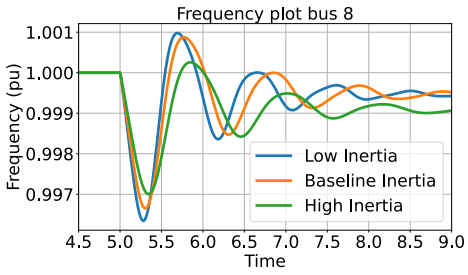

Fig. 7. Frequency plot representing increased and reduced level of inertia during pertubation

B. Impact of Grid-Forming Converters During Lowered Inertia

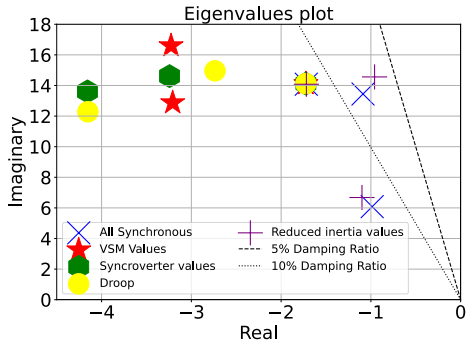

Fig. 8. Eigenvalues plot representing different grid-forming converter additions

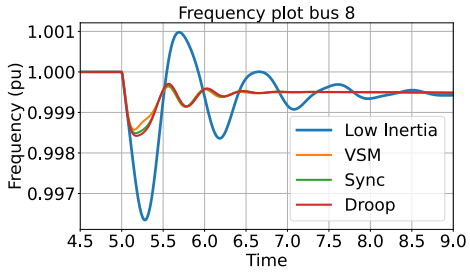

Fig. 9. Frequency plot representing different grid-forming converter additions

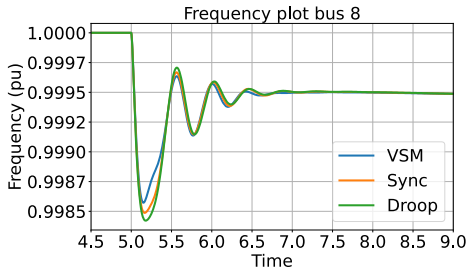

Fig. 10. Frequency plot representing different grid-forming converters

C. Converter Placement Impact

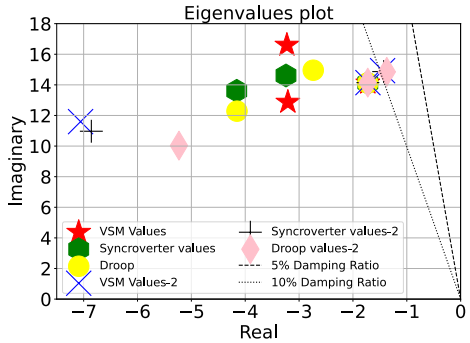

Fig. 11. Eigenvalues plot for comparison of converter placement

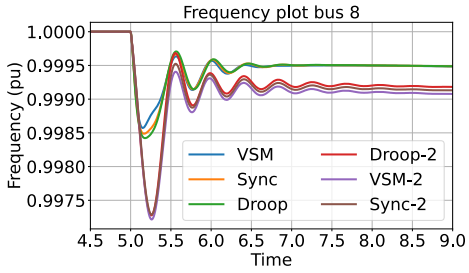

Fig. 12. Frequency plot for comparison of converter placement

D. Parameter Sensitivity Analysis

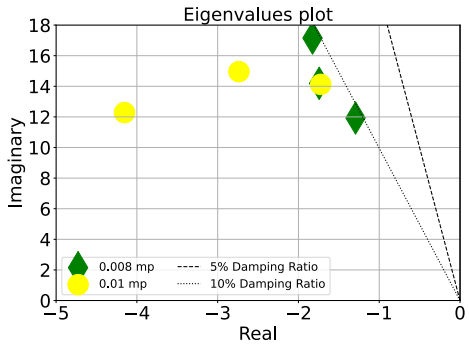

Fig. 13. Eigenvalues plot for comparison of droop coefficient values

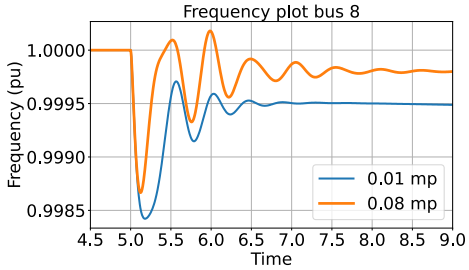

Fig. 14. Frequency plot for comparison of droop coefficient values

V. Analysis of Results

A. Impact of Inertia-changes for Stability

The eigenvalue analysis and frequency response prompted by investigating three distinct inertia scenarios, is depicted in Fig. 6 and 7 respectively. Analysis of the primary three modes, as showcased in Fig. 6, and the incorporation of damping ratios at both 5 % and 10 %, confirms the system's intrinsic stability under all examined conditions—characterized by non-positive real eigenvalues. Yet, a nuanced inspection reveals the tangible influence of varying inertia levels on system stability dynamics.

The eigenvalues highlights that, in comparison to the baseline inertia, simulations with increased and decreased inertia levels manifest an increased oscillatory speed and decreased damping for the first mode under reduced inertia conditions, marked by an increase on the imaginary axis and a decrease on the real axis, respectively. Conversely, an increase in inertia is associated with a decrease in the initial mode's speed alongside an increase in its damping, cumulatively improving the damping ratio for this mode. One mode remains virtually unchanged across the trio of inertia scenarios, whereas the final

mode demonstrates comparable stability attributes between the baseline and increased inertia settings, with the decreased inertia condition exhibiting improved damping alongside an increased speed.

Parallel inferences are noticeable in the frequency response in Fig. 7, where a more substantial inertia endowment is shown to mitigate frequency deviations during the system's initial oscillatory phases, and overall lowered oscillatory response, Indicative of an improved damping ratio as corroborated by the eigenvalue analysis. This synthesis underscores the pivotal role of inertia in modulating the system's oscillatory behavior and stability performance.

B. Oscillatory Dynamics with Grid-forming Converters under Varied Inertia

The impact of grid-forming converters on oscillatory system behavior, particularly under scenarios of low inertia, is depicted through eigenvalue and frequency response analyses, as showcased in Fig. 8 and Fig. 9. The eigenvalue plot, incorporating baseline and reduced inertia states, reveals a uniform influence on modal speed and damping across converter types for one mode, while showcasing divergence in the other two modes. Notably, the minimal modal speeds observed within the converter scenarios are significantly elevated—nearly twofold—relative to the lowest mode in the entirely synchronous settings. This indicates that the integration of grid-forming converters escalates the modal speeds. Nevertheless, these modes exhibit enhanced damping ratios, signaling a system characterized by rapid response and heightened damping efficacy. This observation is reinforced in Fig. 9, where a pronounced reduction in oscillatory behavior and expedited settling times are evident, aligning with the preceding analysis.

Differences in oscillatory performance among the grid-forming converters, albeit subtle, are discernible in Fig. 8. While the distinction between converters is small in comparison to the stabilization effect of their inclusion, nuances exist. For instance, the Droop controller shows an independent mode with marginally lower damping, contrary to the VSM and Syncroverter. Conversely, the Droop controller's final mode exhibits superior damping and reduced speed relative to its counterparts. The VSM and Syncroverter display similar behaviors, albeit with variances in modal speeds. Collectively, all modes under grid-forming control maintain elevated damping ratios, surpassing those associated solely with synchronous generation.

The frequency plots comparing the trio of grid-forming converter implementations further illuminate minor disparities in permissible frequency deviations during oscillations. The VSM emerges as the most responsive, with minimal frequency deviations during both initial oscillations, compared against the Droop's higher deviations, with the Syncroverter intermediating these responses. Despite these slight variations, the transition from purely synchronous generation to a hybrid system incorporating grid-forming converters signifies a pivotal shift towards enhanced modal damping, underscoring the multifaceted impacts of grid-forming converters on system dynamics.

C. Dynamics of Grid-forming Converter Deployment

The strategic positioning of grid-forming converters within the power system infrastructure, specifically the transition from bus 3 alongside generator G3 to bus 10, manifests significant ramifications on damping properties and oscillatory behavior. This is shown through the eigenvalue analysis concerning the principal three modes, given in Fig. 11. Within this analysis, a consistent mode behavior across varied scenarios is observed, albeit with two distinct modes demonstrating notable divergence. One of these modes approaches the critical threshold of the 10 % damping ratio line, marking the lowest damping ratio amongst all modes under each converter configuration at altered locations. The two paramount modes are characterized by relatively modest damping ratios, in contrast to the third mode, which benefits from enhanced damping. However, the aggregate damping efficiency and system speed experiences a decrement, an observation corroborated by the frequency response analysis presented in Fig. 12. The scenarios involving relocated converters exhibit a pronounced increase in permissible frequency deviation during the initial oscillatory phase, underscoring an elevated oscillatory magnitude and protracted settling durations relative to prior configurations, thereby highlighting diminished system damping.

Comparative analyses of converter performance at new deployments mirror findings from preceding evaluations, affirming the nuanced impact of converter placement on system dynamics. This segment underscores the pivotal influence of grid-forming converter positioning on the oscillatory attributes of the power system. Consequently, the strategic deployment of grid-forming converter generation emerges as a critical factor in oscillatory performance enhancement, necessitating meticulous consideration of placement impacts on project-specific stability outcomes. Empirical evidence suggests that converter installation close to or in conjunction with existing synchronous machines may improve stability across various scenarios, particularly in the context of diminishing system inertia. This serves to underscore the imperative for a nuanced analysis of converter placement strategies to optimize stability enhancements within the evolving power system landscape.

D. Converter Parameter Sensitivity and System Dynamics

The sensitivity analysis of converter parameters, as elaborated in section II, shows the nuanced impact of these parameters on system behavior. The analysis finds the acceleration time constant T_a, and the damping coefficient D_q as instrumental for the operational dynamics of both the Virtual Synchronous Machine (VSM) and Syncroverter. Conversely, the voltage control gain K_q and the reactive power droop coefficient D_q manifested minimal influence on the oscillatory performance of the Syncroverter.

A notable observation is the significant influence wielded by the acceleration time constant. Its reduction is directly correlated with heightened oscillatory behavior and protracted settling times, underscoring the criticality of T_a in system stabilization. The interplay of damping levels emerges as a

delicate equilibrium; insufficient damping exacerbates oscillatory magnitudes and settling times, whereas overly aggressive damping poses risks of grid instability through generator pole slippage, as illustrated by pronounced frequency deviations when employing a damping coefficient of 300. In this context, the VSM and Syncroverter exhibit parallel responses to parameter variations.

The Droop controller's sensitivity to active and reactive power coefficients, explored through eigenvalue and frequency response analyses (Fig. 13 and Fig. 14), emphasizes the tangible effects of controller parameter tuning on system oscillatory characteristics. These findings illuminate the potential of strategic controller adjustments to modulate critical system modes. Post-parameter modification, one mode maintains its previous characteristics, whereas the others exhibit a decline in damping ratios, with one mode accelerating and the other decelerating. The frequency response analysis corroborates these observations, indicating that while the Droop adjustment modifies the amplitude of initial oscillations, it concurrently instigates more persistent oscillatory behavior, reflective of diminished modal damping.

Conversely, alterations to the reactive power coefficient exhibit a negligible impact on frequency dynamics and settling intervals, underscoring the inherent linkage between reactive power and voltage stability, rather than frequency stability.

This comprehensive analysis highlights that parameter adjustments within grid-forming converters wield profound implications for the system's oscillatory performance. It underscores the dual role of grid-forming converters in enhancing and potentially compromising system stability, contingent upon the control strategy employed. This revelation accentuates that controller performance across different settings is not a foregone conclusion, advocating for a tailored approach to converter parameter selection to optimize system stability and performance.

VI. Conclusion

The evolving landscape of power systems, propelled by the rise of power electronic interfaced (PEI) generation, demands a reevaluation of stability strategies. Traditional synchronous generators, central to system stability, are being supplemented or replaced by advanced converter technologies. This research explores the operational dynamics of three grid-forming converter topologies: the Virtual Synchronous Machine (VSM), droop control, and the Synchroverter, comparing their performance against conventional synchronous generators under varying inertia conditions.

The study reveals that grid-forming converters can significantly enhance system stability, particularly when positioned close to generators to optimize damping effectiveness in unison with synchronous generators. However, the process of parameter tuning emerges as a critical factor that can compromise stability. Therefore, meticulous calibration is essential for optimizing system stability.

With the increasing integration of PEI generation, grid-forming converter controllers stand out as pivotal in ensuring system stability, despite the inherent challenges. Their strategic implementation and careful parameterization are vital for maximizing their benefits in a renewable-dominant energy landscape.

This investigation provides valuable insights for policy-making, grid development, and the strategic deployment of renewables, contributing a detailed comparative analysis that highlights the role of grid-forming converters in shaping the future of system stability.

References

[1] *Power Electronics for Future Power Grids: Drivers and Challenges*. Alireza Nami. In *2018 20th European Conference on Power Electronics and Applications (EPE'18 ECCE Europe)*, 2018, pp. P.1-P.2.

[2] *A review of concepts in power system stability*. Y. ALShamli, N. Hosseinzadeh, H. Yousef, and A. Al-Hinai. In *2015 IEEE 8th GCC Conference & Exhibition*, Muscat, Oman, 2015, pp. 1-6. [Online]. Available: https://doi.org/10.1109/IEEEGCC.2015.7060093

[3] *Power System Stability with Power-Electronic Converter Interfaced Renewable Power Generation: Present Issues and Future Trends*. Meegahapola, Lasantha, Alfeu Sguarezi, Jack Stanley Bryant, Mingchen Gu, Eliomar R. Conde D., and Rafael B. A. Cunha. In *Energies*, 13, no. 13, 2020: 3441. [Online]. Available: https://doi.org/10.3390/en13133441

[4] *Renewable Energy Prospects for the European Union*. IRENA for EU Union. Published: February 2018. [Online]. Available: https://www.irena.org/-/media/Files/IRENA/Agency/Publication/2018/Feb/IRENA_REmap_EU_2018.pdf

[5] C. Bergamasco, *Denmark meets 100% of its energy needs with wind power alone*, Lifegate, 6 March 2017. [Online]. Available: https://www.lifegate.com/denmark-record-wind-power

[6] Yihui Zuo, Zhao Yuan, Fabrizio Sossan, Antonio Zecchino, Rachid Cherkaoui, Mario Paolone, *Performance assessment of grid-forming and grid-following converter-interfaced battery energy storage systems on frequency regulation in low-inertia power grids*, Sustainable Energy, Grids and Networks, Vol. 27, 2021, pp. 100496, [Online]. Available: https://doi.org/10.1016/j.segan.2021.100496.

[7] X. Gao, D. Zhou, A. Anvari-Moghaddam, and F. Blaabjerg, *A Comparative Study of Grid-Following and Grid-Forming Control Schemes in Power Electronic-Based Power Systems*, AAU Energy, Aalborg University, Aalborg, Denmark, Accepted: 30, November 2022. https://doi.org/10.2478/pead-2023-0001

[8] D. Pattabiraman, R. Lasseter, and T. Jahns, *Comparison of Grid Following and Grid Forming Control for a High Inverter Penetration Power System*, 2018, pp. 1-5. [Online]. Available: https://doi.org/10.1109/PESGM.2018.8586162

[9] Y. Wang, M. Yu, X. Lei, X. Wang, and S. Liu, *Grid-Forming Control of VSC-HVDC for Power Systems with High Proportion of Converter-Based Sources*, 2023 International Conference on Smart Electrical Grid and Renewable Energy (SEGRE), Changsha, China, 2023, pp. 175-180. [Online]. Available: https://doi.org/10.1109/SEGRE58867.2023.00034

[10] B. Bahrani, M. H. Ravanji, B. Kroposki, D. Ramasubramanian, X. Guillaud, T. Prevost, and N.-A. Cutululis, *Grid-Forming Inverter-Based Resource Research Landscape: Understanding the Key Assets for Renewable-Rich Power Systems*, IEEE Power and Energy Magazine, vol. 22, no. 1, pp. 18-29, Mar. 2024. [Online]. Available: https://doi.org/10.1109/MPE.2023.3343338

[11] A. Narula, M. Bongiorno, M. Beza, and P. Chen, *Tuning and evaluation of grid-forming converters for grid-support*, 2021 23rd European Conference on Power Electronics and Applications (EPE'21 ECCE Europe), Ghent, Belgium, 2021, pp. P.1-P.10. [Online]. Available: https://doi.org/10.23919/EPE21ECCEEurope50061.2021.9570679

[12] A. Bakeer, A. Chub, A. Abid, S. A. Zaid, T. A. H. Alghamdi, and H. S. Salama, *Enhancing Grid-Forming Converters Control in Hybrid AC/DC Microgrids Using Bidirectional Virtual Inertia Support*, Processes, vol. 12, no. 1, Article no. 139, 2024. [Online]. Available: https://doi.org/10.3390/pr12010139.

[13] H. Bevrani, T. Ise, and Y. Miura, *Virtual synchronous generators: A survey and new perspectives*, *International Journal of Electrical Power & Energy Systems*, vol. 54, pp. 244–254, 2014. [Online]. Available: https://doi.org/10.1016/j.ijepes.2013.07.009

[14] P. Denholm, T. Mai, R. W. Kenyon, B. Kroposki, and M. O'Malley, *Inertia and the Power Grid: A Guide Without the Spin*, *Technical Report NREL/TP-6A20-73856*, National Renewable Energy Laboratory and University of Colorado Boulder, May 2020. Available: https://www.nrel.gov/docs/fy20osti/73856.pdf

[15] *EE4545 Reader 4*. Prof. José Rueda EWI - TU Delft. 2023. [Online]. Available: https://brightspace.tudelft.nl/d2l/le/content/499770/viewContent/2928193/View. Accessed: 2023-05-03.